JOURNAL OF MATERIALS SCIENCE **38** (2003) 4941 – 4949

Investigations of stiffness and fatigue properties of asphalt mixtures

R. LUNDSTRÖM*, U. ISACSSON, J. EKBLAD
Division of Highway Engineering, Royal Institute of Technology, S-100 44, Stockholm, Sweden
E-mail: Robert.Lundstrom@byv.kth.se
E-mail: Ulf.Isacsson@byv.kth.se
E-mail: Jonas.Ekblad@byv.kth.se

Three conventional asphalt concrete mixtures containing one aggregate of a given size distribution and bitumens of different stiffness obtained from one and the same source are characterised with regard to rheological properties using uniaxial testing. Both non-destructive complex modulus and fatigue testing at different temperatures are performed. The results obtained from the non-destructive testing indicate that the mixtures studied exhibit similar rheological properties (stiffness and phase angle) in the range investigated, if compared at different temperatures (similar rheological state). The results presented also suggest that fatigue deterioration to a great extent is determined by the rheological status of the mixture. Some aspects on the test procedure, such as adequate strain measurement and heating during destructive (fatigue) testing as well as fatigue life characterisation using the classical approach, are discussed. © *2003 Kluwer Academic Publishers*

1. Introduction

During the last decades, increased interest in pavement engineering has been devoted towards more advanced characterisation of asphalt materials based on viscoelastic theory. Generally, asphalt materials are considered to behave linearly viscoelastic under relatively low strain applications. The current trend regarding structural models can be exemplified by VEROAD [1], a linear viscoelastic multi-layer program which permits analysis taking into account both viscoelastic material properties and moving wheel loads. Such models should give more realistic response provided that adequate material and environmental characteristics are available. However, if the resulting strains are sufficiently high, the road materials and, consequently, the entire road structure start to deteriorate.

One main obstacle to analytical design is the lack of laboratory test methods that characterise material properties under practical loading and environmental conditions. In current design procedures, generally fatigue cracking at the bottom of the asphalt layer and permanent deformation at the top of the subgrade are the main distress mechanisms considered. Regarding permanent deformation at the subgrade, both bound and unbound materials contribute. To assess the influence of asphalt material properties on road deterioration, more advanced test methods than presently available are needed. Such methods are characterised by the capability of measuring fundamental parameters at a broad range of conditions.

The objective of the research presented in this paper was to characterise rheological properties of dense-graded asphalt concrete mixtures, manufactured using three conventional bitumens from one and the same source processed to different stiffness. The focus of the study is directed towards determination of rheological behaviour of the mixtures, as characterised by for example stiffness and fatigue, using uniaxial testing. The non-destructive testing includes more than 30 complex modulus tests performed at different temperatures and frequencies and the fatigue tests almost 100 strain- or stress-controlled tests at different temperatures and amplitudes. The fatigue investigation concerns high cycle fatigue tests (large number of load applications to failure), and the results are presented using the classical fatigue (Wöhler) approach. In a subsequent paper [2], a viscoelastic continuum damage model is used to further analyse the fatigue results presented in this paper.

2. Experimental

2.1. Materials

In Sweden, ABT mixtures (dense-graded asphalt concrete) are the most common materials used as wearing and binder courses. ABT mixtures are continuously graded and can consist of different penetration grade bitumens in order to account for different field

*Author to whom all correspondence should be addressed.

TABLE I Penetration and softening point of the recovered bitumen

Bitumen	50/60	70/100	160/200
Penetration (25°C, mm/10)	42	60	139
Softening point R&B (°C)	53.3	50.6	42.0

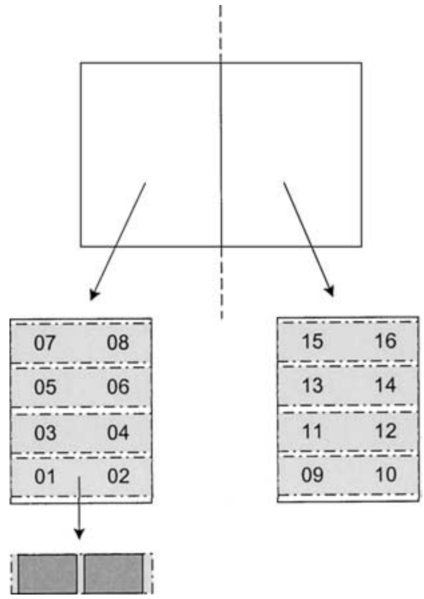

Figure 2 Specimen preparation procedure.

160/220 A

2.5	1.6	2.0	3.4
1.8	1.4	1.3	2.1
1.9	1.3	1.2	1.9
2.7	1.4	1.5	3.2

160/220 B

3.5	2.2	2.0	3.4
2.4	1.5	2.0	3.1
2.4	1.5	1.9	2.6
2.3	1.6	2.0	4.0

70/100 A

4.0	2.8	2.1	3.7
3.0	1.6	1.7	2.8
2.6	1.7	1.8	2.0
3.5	2.4	2.4	3.5

70/100 B

4.3	2.7	1.9	3.9
2.9	1.8	1.3	2.5
2.2	1.3	1.5	2.6
3.1	1.9	2.2	4.1

50/60 A

2.6	1.6	1.6	3.2
1.8	1.5	1.4	2.1
2.1	1.7	1.4	2.2
3.1	1.9	1.4	2.5

50/60 B

4.0	2.5	2.1	4.4
2.4	1.5	1.7	2.5
2.4	1.2	1.4	2.5
3.6	1.5	1.3	3.0

Figure 3 Air void contents (% by volume) of each specimen.

conditions, e.g., amount of heavy traffic and climate. In this study, a wearing course mixture with maximum aggregate size 11 mm, i.e., ABT 11, was used. The aggregate consisted of typical Swedish crushed granite (Farsta Granite). Three conventional bitumens with penetration grade 50/60, 70/100 and 160/220, respectively, were employed in this investigation. The numbers indicate penetration grade range at 25°C in mm/10. The source of the bitumen was Laguna, Venezuela, and the bitumen was provided by Nynäs AB. The penetration and softening point values of the recovered binders are shown in Table I.

According to Swedish road standards [3], an ABT 11 mixture may consist of different penetration grade bitumen as already mentioned. However, the binder content depends on the binder grade used. Therefore, in order to make a meaningful comparison of the influence of binder stiffness on mechanical response, the same target binder content was chosen for all three mixtures studied (6.2% by weight). The target air void content was 3.4 ± 1 (% by volume). These targeted levels were checked by measurements. The measured particle size distribution of the aggregate as well as the limits according to [3] is shown in Fig. 1.

The mixtures were manufactured at Nynäs AB in Nynäshamn, Sweden, and compacted to slabs using a laboratory rolling wheel compactor (MAP, Spechbach-le-bas, France). The final dimensions of each slab were $150 \times 295 \times 600$ mm. In total, 6 slabs, two of each mixture, were manufactured for testing. Each slab was sawn in halves, four 30 cm cylinders ($\phi = 80$ mm) were cored from each half, and the cores were sawn into two samples of desired length ($h = 120$ mm) (Fig. 2).

Fig. 3 shows the measured air void content of the specimens from each slab. It can be seen, that the void content of each specimen is normally 1–4% (by volume). Normally, the highest void contents are obtained at the corners of the slabs.

The differences in single values are apparently large. However, the testing, as described in Chapter 3, do not indicate, that such a range in void content influences the results significantly. By ANCOVA (analysis of covariance) analysis it was also shown that the air void content did not affect the rheological behaviour as determined from the complex modulus measurements in a significant way.

2.2. Testing equipment and program

The specimens described in Section 2.1 were investigated using unconfined uniaxial testing. The test set-up (Fig. 4) was the same for both complex modulus and fatigue tests and consisted of a servo-hydraulic testing system (MTS 810, Teststar II).

The axial deformations were measured using three MTS strain-gauge extensometers, placed 120° from each other and connected with springs around the middle of the sample. The gauge length was chosen to 50 mm to avoid end effects close to the end-caps due to the gluing.

During all complex modulus tests, the specimens were subjected to a sinusoidally oscillating axial loading (no rest period) in both tension and compression (through zero) at constant $50 \cdot 10^{-6}$ m/m strain

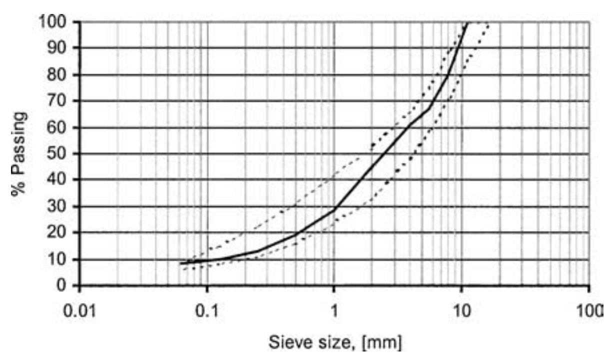

Figure 1 Measured particle size distribution of the aggregate used and the limits according to [3].

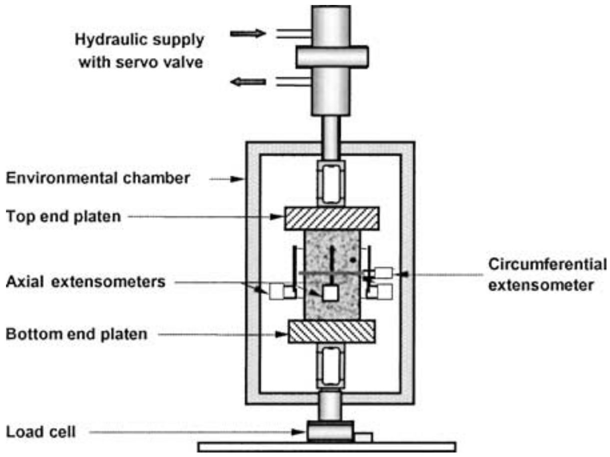

Figure 4 Testing set-up for complex modulus and fatigue tests.

amplitude. The complex modulus tests were considered to be non-destructive, thus allowing subsequent fatigue testing. The applied strain amplitude was kept low (i.e., $50 \cdot 10^{-6}$ m/m) in order to avoid damaging the material but high enough to avoid equipment related data measuring limitations. All materials were tested at four temperatures (0, 10, 20 and 30°C) and 9 frequencies (40, 32, 16, 8, 4, 2, 1, 0.5 and 0.1 Hz). A second measurement at 40 Hz was also performed in order to observe, if any damage had occurred. During the tests, the mean value of the three extensometers was controlled. Consequently, the tests were "true" strain controlled tests, since the measured strains are not only recorded but also used as indata for machine control. The load and displacement amplitudes at complex modulus testing were determined using Fourier analysis over eight cycles recorded. The Fast Fourier Transform (FFT) technique has the advantage to detect and filter spurious effects of harmonics and noise in the signal, allowing an indication of the quality of the filtered signal by the ratio between amplitude of the fundamental frequency component and the sum of amplitudes of all the frequency components generated. The average ratios during the trials were generally high, and occurring deviation may be explained by material inhomogeniety, nonlinearity and configuration factors of the test equipment.

During the fatigue tests, the specimens were subjected to a sinusoidally oscillating axial loading (no rest period) in both tension and compression (through zero) at three different temperatures 0, 10, 20°C and always at frequency 10 Hz. The tests were performed in both controlled stress and controlled strain modes. The loading amplitudes were chosen in such a way that the fatigue life would be in the range of 80,000 to 1 million cycles. At least two samples were performed at each test condition. Stress and strain amplitudes were determined using FFT over four cycles. The reason for choosing only four cycles instead of the eight used in the complex modulus tests is a compromise between reliable parameter determination and detailed knowledge of its evolution. During the tests, the data were recorded heavily at the beginning but were later recorded less frequently in order to obtain sufficient but still manageable data. During the fatigue tests, the increase in sample temperature was recorded on the envelope surface of each specimen using a thermocouple. During all complex modulus and fatigue tests, Poisson's ratio was measured using a chain linked to an extensometer (cf. Fig. 4).

The rheology of recovered binders was investigated using both conventional tests (penetration and softening point) and more fundamental tests by a dynamic shear rheometer (RDA-II, Rheometrics Inc.).

3. Results and analysis

3.1. Complex modulus tests

Complex modulus tests refer to non-damaging rheological characterisation of linear viscoelastic material properties under periodic sinusoidal loading. The test provides parameters such as dynamic modulus, phase angle and time-temperature shift factors. In the reminder of analysis, engineering stress σ and strain ε are employed as nominal values, i.e.,

$$\sigma = \frac{P}{A} \tag{1}$$

$$\varepsilon = \frac{u}{L} \tag{2}$$

where P is the load over initial cross-sectional area, A, and related to the displacement, u, measured over initial gauge length, L. The complex modulus is the representation of the modulus of a viscoelastic material as the sum of the real and imaginary parts

$$E^* = E' + iE'' \tag{3}$$

or in polar form

$$E^* = |E^*|e^{i\phi} \tag{4}$$

where $|E^*|$ is the dynamic modulus defined as the ratio between the amplitudes of stress and strain signals

$$|E^*| = \frac{\sigma_0}{\varepsilon_0} \tag{5}$$

and ϕ is the phase angle obtained as

$$\phi = \tan^{-1}\left(\frac{E''}{E'}\right). \tag{6}$$

In a similar way, constitutive equations describing the response of a linear viscoelastic material under periodic shear will lead to the definition of dynamic shear modulus, $|G^*|$, and corresponding phase angle, φ, respectively.

Generally, viscoelastic materials exhibit both temperature and time (or frequency) dependence. Bituminous binders and mixtures are normally referred to as thermorheologically simple, which means that the construction of master curves from horizontally shifted isotherms is possible (cf.Fig. 5).

Consequently, the dependence of the material property upon (angular) frequency, ω, and temperature, T, can be represented solely by a single parameter, reduced frequency, ζ, which at constant temperature is obtained as

$$\zeta = \omega \cdot a_T \tag{7}$$

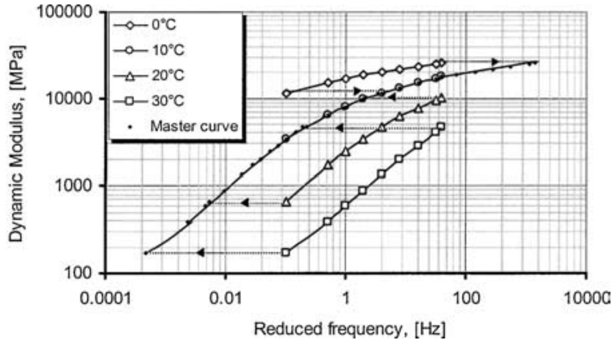

Figure 5 Example of a master curve for dynamic modulus obtained using the time-temperature superposition principle (70/100 mixture).

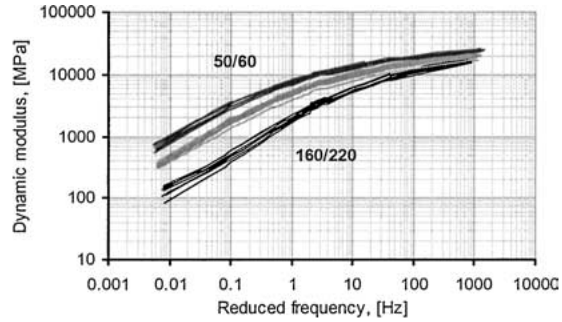

Figure 7 Master dynamic modulus curves for the three materials studied.

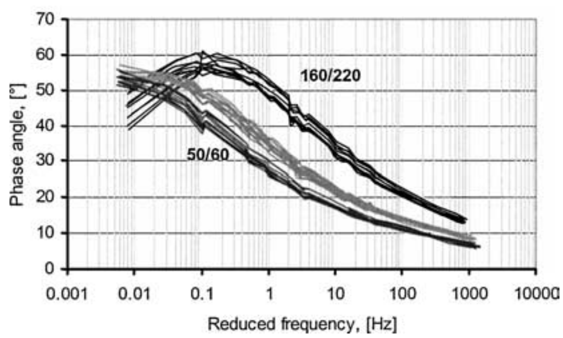

Figure 8 Phase angle curves of the mixtures studied.

For thermorheologically simple materials, it is often convenient to analytically express the shift factor using the WLF (Williams-Landell-Ferry) equation

$$\log a_{\mathrm{T}} = -\frac{C_1(T - T_0)}{C_2 + T - T_0} \tag{8}$$

where C_1 and C_2 are constants, T and T_0 are temperature and reference temperature, respectively. Equation 8 provides the possibility to interpolate rheological properties at any temperature.

3.1.1. Binders

The dynamic shear modulus $|G^*|$ and phase angle φ data of recovered binders are shown in Fig. 6. As can be seen, the difference between the three curves is small. The overall results suggest that the binder manufacturing process does not significantly change the rheological relationships as described by these two parameters (dynamic shear modulus and phase angle) for the different penetration grades studied.

3.1.2. Mixtures

The rheological characterisation of the mixtures was carried out by complex modulus testing on at least two specimens from each slab-half. The resulting dynamic modulus and phase angle mastercurves from all complex modulus tests of the mixtures are shown in Figs 7 and 8.

Fig. 7 shows all master dynamic modulus curves for the three mixtures. In total 10–14 samples from each mixture are displayed. The three materials are well gathered in three distinct groups, suggesting significant differences between the materials containing bitumen of different stiffness. Within each group, the differences in stiffness at a given frequency are within 5–10% which is considered relatively small. The highest stiffness is obtained with the 50/60 mixture, while the 160/220 mixture shows the lowest stiffness at a given reduced frequency. A similar comparison is shown in Fig. 8, where all master phase angle curves are displayed. The 160/220 mixture shows the highest phase angle for a given frequency, while the 50/60 mixture shows the lowest. For phase angles corresponding to reduced frequencies lower than 0.1 Hz, a peak is observed. This peak is believed to be the result of increased relative importance of the aggregate skeleton at soft conditions.

Fig. 9 shows the properties of the mixtures in form of a Black diagram. As in the case of the binders (cf. Fig. 6), it can be seen that the different materials exhibit almost the same relationship between dynamic modulus and phase angle over the whole range, suggesting the materials are very similar. However, it should be noted that the influence of temperature is not explicitly shown in this type of diagram.

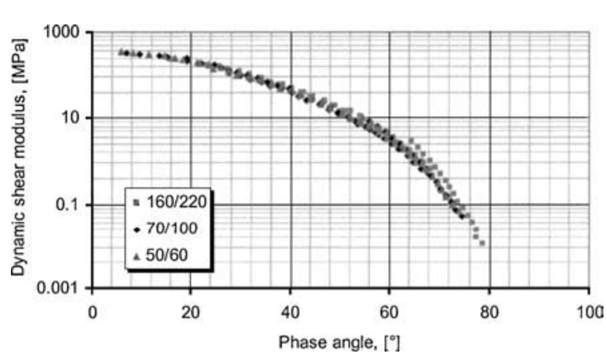

Figure 6 Black diagram showing dynamic shear modulus vs. phase angle for the 50/60, 70/100 and 160/220 binders.

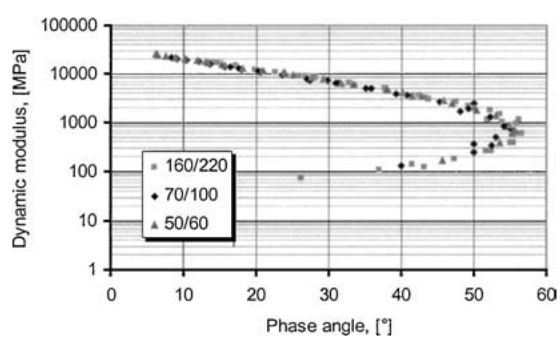

Figure 9 Black diagram for the three mixtures studied.

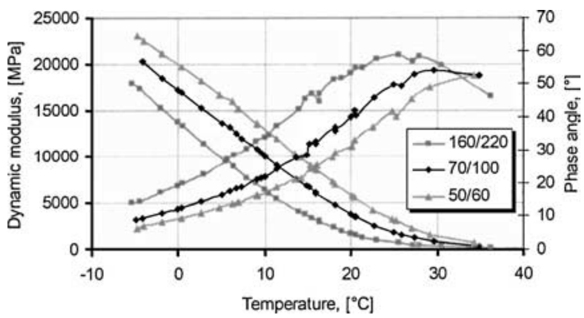

Figure 10 Isochrones for the three mixtures (shifted to frequency 10 Hz).

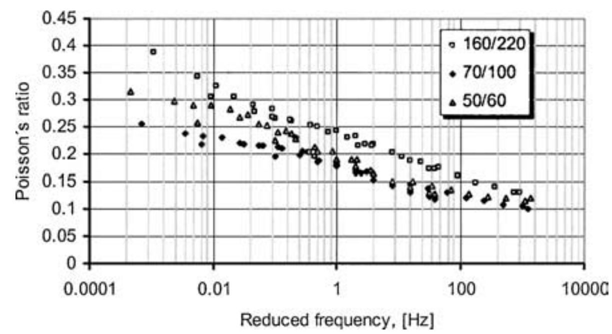

Figure 11 Poisson's ratio as a function of reduced frequency for the three mixtures studied. Reference temperature 10°C.

In order to provide information regarding influence of temperature on rheological properties of the three mixtures, each material is shifted to frequency 10 Hz using the WLF equation (Equation 8). Fig. 10 shows the resulting isochrones of the materials. It can be seen, that there are large differences between the three materials in terms of dynamic modulus and phase angle for each temperature.

According to Fig. 10, the differences between the 50/60 and 160/220 materials are close to 10°C over the whole temperature range.

The dynamic modulus of the 50/60 mixture at 10°C is approximately 13,000 MPa, which is almost the same as for the 160/220 mixture at 0°C. At 20°C, the dynamic modulus of the 50/60 is of the same order of magnitude as the 160/220 mixture at 10°C. A similar relationship can be found for the phase angles. These results are interesting, since the fatigue characterisation described in Section 3.2 is carried out at 0, 10 and 20°C for all mixtures, providing opportunity to compare fatigue characteristics at similar initial stiffness and phase angle. In other words, if fatigue test results are similar for the 50/60 mixture at 10°C and the 160/220 mixture at 0°C, the rheological properties only depend on the current rheological state of the materials and not on possible physical or chemical differences between the binders. The ability of results obtained at different times or temperatures to fit onto a single master curve is often referred to as thermorheological simplicity. As shown above, different penetration grade bitumens may lead to asphalt mixtures exhibiting similar rheological properties at a certain combination of time and temperature. Table II shows representative shift factors obtained for the mixtures.

TABLE II Shift factors of the mixtures investigated

Mixture	Temperature (°C)	a_T
50/60	0	35.1
	10	1.00
	20	0.055
	30	0.005
70/100	0	30.9
	10	1.00
	20	0.064
	30	0.007
160/220	0	23.0
	10	1.00
	20	0.093
	30	0.011

Another important parameter obtained during complex modulus measurements is Poisson's ratio, which is obtained by relating the transverse, ε_T, and axial strain, ε_A, of the test specimen submitted to axial deformations. In classical theory, Poisson's ratio is between 0 and 0.5. According to [1], Poisson's ratio for asphalt mixtures depends on temperature, frequency and applied strain amplitude (cf. Equation 9)

$$\upsilon^* = -\frac{\varepsilon_T}{\varepsilon_A} e^{i(\phi - \varphi)} \approx \frac{\varepsilon_T}{\varepsilon_A} \tag{9}$$

where ϕ and φ are the phase angle of the axial and transverse phase angle, respectively. However, as these two phase angles are essentially the same, Poisson's ratio can be treated as a real number.

As in the case of dynamic modulus, Poisson's ratio can be expressed as a mastercurve. Fig. 11 shows typical master curves for the three mixtures as determined by complex modulus tests. The shift factors used were those obtained from the corresponding complex modulus test. It was observed that relatively large differences between different samples as well as large scattering among data occurred for many tests. This is indicated in Fig. 11 where the ranking is not consistent with other master curves; the 50/60 mixture exhibits Poisson's ratio between those of the 70/100 and 160/220 mixtures. These effects are probably due to the test set-up. Due to the difficulties addressed, careful evaluation of Poisson's ratio is necessary.

The results show that softer conditions exhibit higher Poisson's ratios. The range in Poisson's ratio obtained in this investigation is 0.1 to 0.4, which is smaller than earlier reported by [4, 5]. The difference may be explained by the fact that an amplitude of only $50 \cdot 10^{-6}$ m/m was used in this study.

3.2. Fatigue tests

3.2.1. Evolution of stiffness

According to Di Benedetto *et al.* [6], a typical fatigue process for asphalt mixtures can be characterised by three distinct phases denoted Phase I, II and III, respectively. The first phase is characterised by a rapid increase in sample temperature. During this phase, the stiffness of the sample decreases due to both fatigue damage and temperature increase. The effect of heating is very difficult to separate from the fatigue damage during Phase I and therefore difficult to analyse. Phase II is characterised by a quasi-linear decrease in stiffness. At

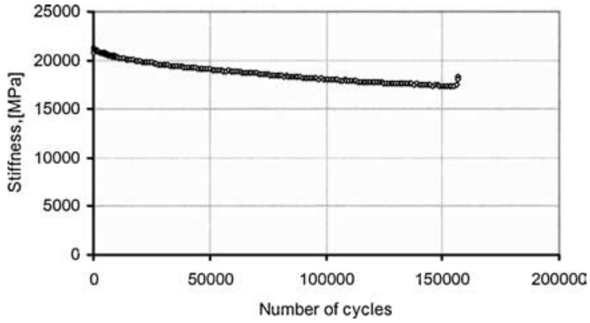

Figure 12 Evolution of stiffness during a controlled strain (100 $\mu\varepsilon$) fatigue test at 0°C using the 50/60 mixture.

the beginning of the Phase III, the sample starts to collapse, often due to increased non-uniformity in strain field. The behaviour during such a three-step evolution of the stiffness can be very different for different temperatures and binder stiffness used. The fatigue testing in this study covered an overall range of initial stiffness of 1,800–21,000 MPa (cf. Figs 12–14). As in the case of the complex modulus tests, the repeatability of different tests is comparatively high, and often show very similar initial stiffness as well as deterioration path.

For the mixture consisting the stiffest binder (50/60) at 0°C, the stiffness generally did not decrease more than in total 15–20% before final failure (cf. Fig. 12), which suggests that Phase 1 is very small under this condition. However, it was noticed that Phase 1 seems slightly more important for 70/100 and 160/220 mixtures at 0°C. Phase 3 was easily identified for most tests at 0°C due to the distinct failure (cf. Fig. 12).

The fatigue behaviour of the mixtures changed in some respects, when the temperature increased from 0 to 10°C. The initial stiffness of the mixtures decreased

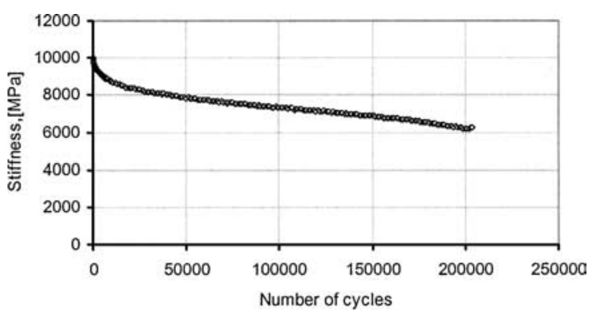

Figure 13 Evolution of stiffness for the 70/100 mixture during controlled strain (100 $\mu\varepsilon$) fatigue test at 10°C.

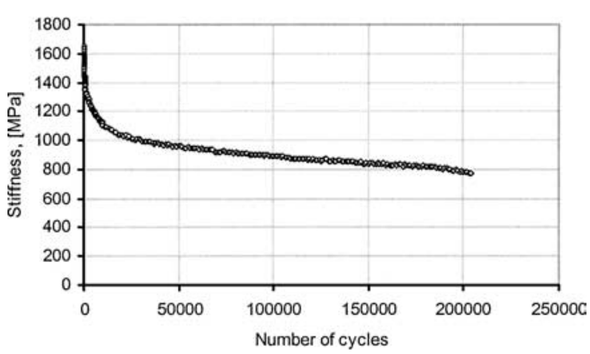

Figure 14 Evolution of the stiffness of the 160/220 mixture at controlled strain (300 $\mu\varepsilon$) fatigue test at 20°C.

in accordance with expected decrease obtained from complex modulus tests. In general, the initial stiffness of all fatigue tests showed similar values as obtained from dynamic modulus tests (cf. Fig. 10), i.e., no strain dependent non-linear behaviour was observed. Fig. 13 shows the evolution of the stiffness for the 70/100 mixture at 10°C. The first phase described by [6] is much more pronounced compared to that at 0°C for the same material. The rapid reduction in stiffness during Phase 1 becomes almost linear during Phase 2. In most cases, the stiffness decreased about 40% of its initial value before complete failure. However, it is observed that there are relatively large differences in failure point expressed in stiffness between different samples.

It should also be noted that the relative decrease in stiffness ($E_{\text{Failure}}/E_{\text{Initial}}$) also increases with increased temperature. The fatigue tests carried out at 10°C generally sustained a larger decrease in stiffness before the start of Phase 3 compared to stiffer conditions. This phenomenon may be due to relaxation and temperature increase through hysteresis heating. The fatigue tests carried out at 20°C followed the same trend as already described for the lower testing temperatures. The initial reduction in stiffness was around 40% for the 160/220 mixture before stabilising as indicated in Fig. 14. When comparing fatigue tests of the 50/60 and 160/220 mixtures at a temperature difference of 10°C, results indicate that deterioration processes are similar at a given strain amplitude.

The examples and reflections described above relate only to controlled strain fatigue tests. It can be seen, that the decrease in stiffness in general is regressive. However, there are exceptions. For all stress-controlled tests, the regressive decrease rate reaches an inflexion point, after which it becomes progressive, i.e., the decrease in stiffness starts to accelerate and the stiffness curve becomes S-shaped (cf. Fig. 15).

The reason for the S-shaped behaviour often obtained for stress-controlled fatigue tests is due to the fact that the strain amplitude increases continuously during the test but also due to an accelerating heating (cf. Section 3.2.3). When controlled strain tests show this type of deterioration curve, it is usually due to a non-uniform strain field [7].

3.2.2. Poisson's ratio

Poisson's ratio was investigated during the fatigue tests in the same way as at complex modulus testing. It was

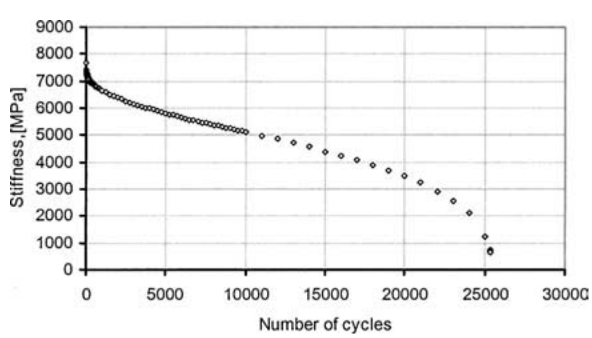

Figure 15 Typical S-shaped stiffness curve obtained in controlled stress (1.6 MPa) fatigue test at 20°C (50/60 mixture).

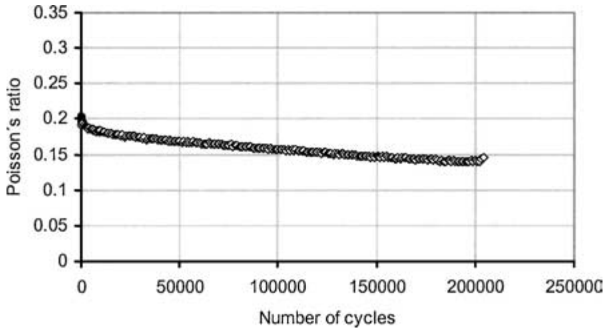

Figure 16 Evolution of Poisson's ratio of the 70/100 mixture at controlled strain (100 $\mu\varepsilon$) fatigue test at 10°C.

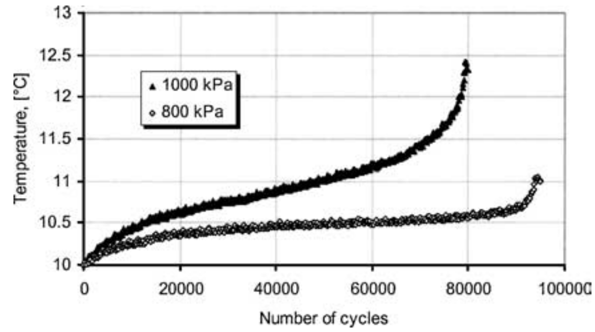

Figure 17 Temperature increase during two controlled stress tests of the 70/100 mixture at 10°C.

observed that the evolution of Poisson's ratio varies with the mode of loading. Poisson's ratio generally decreases during strain-controlled tests (cf. Fig. 16). The decrease rate is dependent on the strain amplitude; i.e., the higher the strain amplitude, the faster the decrease. The initial value is related to the stiffness of the mixture and corresponds to Poisson's ratio as obtained from complex modulus testing.

According to [1], Poisson's ratio is strain amplitude dependent, which was also generally observed in this study: the higher the strain amplitude, the higher Poisson's ratio. This trend was also observed for all test conditions, but the differences between replicates were relatively large compared to dynamic modulus results. This may be explained by the measurement procedure, which seems to be more sensitive due to use of chain. During stress controlled tests, the evolution in Poisson's ratio is more or less linear in time, i.e., no strain dependence could be observed.

3.2.3. Increase in temperature

During fatigue tests, the increase in temperature was recorded on the envelope surface of each sample using a thermocouple. The evolution in temperature for the two modes of loading was similar to those reported by [8]. The heating measured in controlled strain tests reached a maximum at approximately 30,000–50,000 cycles for all mixtures and temperatures. After passing the peak, the temperature decreases slowly, depending on strain level. The peak increase in temperature depends on stiffness and strain level (i.e., energy input) but was for the controlled strain tests performed in this study often less than 1°C.

For controlled stress tests, the evolution in temperature was increasing throughout the test. The temperature evolution was similar to a creep curve, comprising the primary, secondary and tertiary stages. At failure, the increase in temperature was up to 3°C, depending on stress level, stiffness and testing temperature. Such a high global temperature increase significantly affects the stiffness of the mixture as indicated in Fig. 10, where one degree increase in temperature results in a global decrease in stiffness of approximately 7% of the 70/100 mixture at 10°C. Fig. 17 shows the increase in temperature during two fatigue tests at 10°C. In the tertiary stage, the temperature increases very rapidly, causing the stiffness decrease to accelerate. It was observed that the tertiary stage was in the order of 10 to 25% of total fatigue testing time. This large increase in temperature may influence the shape of the stiffness decrease curve, and thereby contribute to determination of fatigue characteristics such as damage rate (when stiffness reduction is used as a measure of damage) as well as subsequent failure. Furthermore, the effect of heating on the microscale is probably higher, since the dissipated energy responsible for the heat produced is solely generated in the viscoelastic matrix, which only accounts for roughly 5% of the total mixture.

4. Fatigue life evaluation based on classical analysis

Fatigue results are normally obtained using power relationships such as

$$N_{\mathrm{f}} = a \cdot \varepsilon^{\mathrm{b}} \tag{10}$$

where a and b are experimentally determined constants, and N_{f} is the number of load cycles applied until failure at a given strain amplitude, ϵ. The failure is usually arbitrarily defined as the 50% decrease in initial stiffness [9, 10]. This way of expressing fatigue characteristics of an asphalt mixture is common, since it provides a simple way of discriminating between different mixtures and test conditions, e.g., temperatures, loading times and patterns. In Table III, results obtained using Equation 10 (controlled strain tests) are presented. The results in Table III imply that softer binder and higher temperature result in longer fatigue life at a given strain amplitude. However, as discussed below, the classical analysis shows several drawbacks.

TABLE III Fatigue results obtained based on classical analysis

Materials	Temperature (°C)	N_{f} (50%) a	b	R^2
50/60	0	2.97×10^{12}	−3,51	0,76
	10	9.36×10^{15}	−5,18	0,71
	20	4.31×10^{12}	−3,51	0,45
70/100	0	3.61×10^{16}	−5,72	0,58
	10	2.54×10^{16}	−5,42	0,67
	20	1.08×10^{27}	−9,71	0,46
160/220	0	5.17×10^{14}	−4,71	0,52
	10	1.05×10^{12}	−3,04	0,30
	20	1.10×10^{16}	−4,45	0,86

As shown in Table III, some R^2 values are very low, indicating large scatter among the test results. Table III also indicates that the constants a and b vary significantly with testing temperature. This temperature dependence results in the need of extensive testing to obtain constants for several test conditions, if reliable analysis is to be carried out. The large differences shown in Table III are not surprising but stress the importance of accounting for, not only the stiffness of the material, but also its fatigue deterioration properties at a given temperature.

As described in Section 3.2.3, hysteretic heating may significantly influence rheological characteristics of asphalt materials subjected to cyclic loading. It is not clear how to account for this heating using classical analysis, and, consequently, further research is needed in order to determine the magnitude of this effect, and to model it.

A third major problem related to fatigue characteristics using Equation 10 is the fact that, in practice, it is difficult to define failure. As described in Section 3.2.1, failure often occurs suddenly by a rapid drop in global stiffness, and the criterion is met when stiffness passes the 50% decrease level. It is doubtful if such a criterion is meaningful for adequate modelling and prediction of fatigue deterioration of asphalt materials.

The above discussed limitations in asphalt fatigue analysis using the classical approach makes it difficult to evaluate, and, consequently, compare asphalt materials. As described in Section 3.1.2, the differences between the 50/60 and 160/220 materials correspond to 10°C over the whole temperature range investigated. This finding is not supported by the results shown in Table III. However, by the use of continuum damage theory [2], it was shown that this relationship is also applicable to fatigue deterioration.

5. Conclusions

The main findings based on the results presented in this paper can be summarised as follows:

5.1. Methodology

- The use of laboratory compacted slabs is considered to be an appropriate method for manufacturing specimens for rheological (including fatigue) characterisation.
- Uniaxial testing provides reliable characterisation of rheological properties of asphalt mixtures subjected to small and large strains.
- The use of three parallel extensometers greatly improves the information regarding the deterioration process under fatigue testing. The on-sample measurement makes it possible to monitor the decrease in stiffness as well as damage accumulation, but also disturbances in the strain field. The uniformity of the applied strain field is an essential factor when evaluating fatigue characteristics, as non-uniformity may lead to incorrect interpretation of the results.
- Poisson's ratio is an important parameter for structural analysis of flexible pavements. However, the present way of measuring radial strains using a relatively long chain connected to the extensometer does not seem to be optimal, and consequently, further development in this area is desirable.
- The use of thermocouples to monitor increase in temperature during fatigue testing is recomended.

5.2. Rheology

- Mixtures containing aggregate of a given size distribution and manufactured from conventional binders obtained from one and the same source but of different penetration grade show similar behaviour when compared at the same rheological state, i.e., when exhibiting the same dynamic modulus and phase angle. This result means that influence of different binder stiffness on mixture rheology may be modelled using simply a shift factor. However, this conclusion needs to be confirmed for binders from other sources than the one used in this study. The differences between the 50/60 and 160/220 mixtures studied, at 10 Hz, correspond to a difference in temperature of approximately 10°C.
- The specimen air void content variance observed does not significantly influence the stiffness of the materials.
- At analysis of road structures, a time and temperature dependent Poisson's ratio should be used. However, this conclusion is based on relatively large scattered and not always consistent results, and for that reason more research is needed.
- The influence of hysteresis heating should not be underestimated, especially when controlled stress fatigue tests are analysed; stress-controlled fatigue tests often showed high temperature increase (up to 3°C) before failure.
- The classical fatigue evaluation method used in this paper shows many shortcomings. The high scattering among fatigue data and the large amount of tests necessary to cover a given temperature range leads to requirement of several samples and repetitions for adequate characterisation. It is not possible to compare strain- and stress-controlled test results using the classical approach. The 50% reduction in stiffness is not a good failure criterion, since failure tends to occur at different residual stiffness depending on initial stiffness and testing temperature used. The classical failure criterion (50% reduction in stiffness), leads to inconsistent fatigue results and are, consequently, of limited value when applied to structural analysis of flexible pavements.

Acknowledgement

The study described in this paper was carried out with financial support from the Swedish National Board for Industrial and Technical Development (NUTEK), today part of Swedish Agency for Innovation Systems (VINNOVA), through the Road/Bridge/Tunnel (Väg/Bro/Tunnel) consortium. Nynäs AB is greatly acknowledged for providing testing materials.

References

1. R. NILSSON, "Viscoelastic Pavement Analysis Using VEROAD," Ph.D. thesis, Royal Institute of Technology (KTH), Stockholm, Trita-IP FR 01-91, 2001.

2. R. LUNDSTROM and U. ISACSSON, “Modelling Asphalt Fatigue Using Continuum Damage Theory,” submitted for publication, 2002.
3. ATB VÄG, “General Technical Construction Specifications for Roads,” Swedish National Road Administration, Borlänge, 2000.
4. G. SAYEGH, “Viscoelastic Properties of Bituminous Mixtures,” in Proc. 2nd International Conference on Structural Design of Asphalt Pavements (Ann Arbor, MI, USA, University of Michigan, 1967).
5. E. DOUBBANEH, “Comportement Mécanique des Enrobes Bitumineux des Petites aux Grandes Deformations,” Ph.D thesis, INSA-ENTPE, 1995.
6. H. DI BENEDETTO, A. SOLTANI and P. CHAVEROT, *J. Assoc. Asph. Pav. Techn.* **65** (1996) 142.
7. R. LUNDSTROM, “Rheological and Fatigue Characterisation of Asphalt Concrete Mixtures Using Uniaxial Testing,” Licentiate thesis, Royal Institute of Technology (KTH), Stockholm, TRITAVT FR02:02, 2002.
8. A. SOLTANI, “Comportement en fatigue des enrobés bitumineux,” Ph.D thesis, INSA-ENTPE, Lyon, 1998.
9. J. JUDYCKI, “Fatigue of Asphalt Mixes,” University of Oulu, Publications of Road and Transport Laboratory, Finland, 1991.
10. H. DI BENEDETTO and C. DE LA ROCHE, in “State of the Art on Stiffness Modulus and Fatigue of Bituminous Mixtures,” Rilem Report 17, Bituminous Binders and Mixtures, edited by L. Francken (E&FN Spon, London, 1998).

Received 10 October 2002
and accepted 18 August 2003